Article

Cancer Cell

Dysfunction of the Reciprocal Feedback Loop between GATA3- and ZEB2-Nucleated Repression Programs Contributes to Breast Cancer Metastasis

Highlights

- GATA3 is physically associated with the G9A/NuRD(MTA3) complex
- The GATA3/G9A/NuRD(MTA3) complex represses ZEB2
- The GATA3/G9A/NuRD(MTA3) complex suppresses the metastasis of breast cancer
- The ZEB2/G9A/NuRD(MTA1) complex represses G9A and MTA3

Authors

Wenzhe Si, Wei Huang, ..., Yan Wang, Yongfeng Shang

Correspondence

yanwang@tmu.edu.cn (Y.W.), yshang@hsc.pku.edu.cn (Y.S.)

In Brief

Si et al. show that GATA3 interacts with G9A and the NuRD (MTA3) complex to transcriptionally repress genes involved in epithelial-to-mesenchymal transition. Dysfunctional reciprocal feedback regulation between GATA3/G9A/NuRD(MTA3) and ZEB2/G9A/NuRD(MTA1) contributes to breast cancer progression.

Accession Number

GSE67206

Si et al., 2015, Cancer Cell *27*, 822–836
June 8, 2015
http://dx.doi.org/10.1016/j.ccell.2015.04.011

CellPress

CellPress

Cancer Cell
Article

Dysfunction of the Reciprocal Feedback Loop between GATA3- and ZEB2-Nucleated Repression Programs Contributes to Breast Cancer Metastasis

Wenzhe Si,[1] Wei Huang,[2] Yu Zheng,[2] Yang Yang,[2] Xujun Liu,[1] Lin Shan,[2] Xing Zhou,[2] Yue Wang,[2] Dongxue Su,[2] Jie Gao,[2] Ruorong Yan,[1] Xiao Han,[1] Wanjin Li,[1] Lin He,[1] Lei Shi,[2] Chenghao Xuan,[2] Jing Liang,[1] Luyang Sun,[1] Yan Wang,[2,*] and Yongfeng Shang[1,2,*]

[1]Key Laboratory of Carcinogenesis and Translational Research (Ministry of Education), Beijing Key Laboratory of Protein Posttranslational Modifications and Cell Function, Department of Biochemistry and Molecular Biology, Peking University Health Science Center, Beijing 100191, China

[2]2011 Collaborative Innovation Center of Tianjin for Medical Epigenetics, Tianjin Key Laboratory of Medical Epigenetics, Department of Biochemistry and Molecular Biology, Tianjin Medical University, Tianjin 300070, China

*Correspondence: yanwang@tmu.edu.cn (Y.W.), yshang@hsc.pku.edu.cn (Y.S.)

http://dx.doi.org/10.1016/j.ccell.2015.04.011

SUMMARY

How loss-of-function of GATA3 contributes to the development of breast cancer is poorly understood. Here, we report that GATA3 nucleates a transcription repression program composed of G9A and MTA3-, but not MTA1- or MTA2-, constituted NuRD complex. Genome-wide analysis of the GATA3/G9A/NuRD(MTA3) targets identified a cohort of genes including ZEB2 that are critically involved in epithelial-to-mesenchymal transition and cell invasion. We demonstrate that the GATA3/G9A/NuRD(MTA3) complex inhibits the invasive potential of breast cancer cells in vitro and suppresses breast cancer metastasis in vivo. Strikingly, the expression of GATA3, G9A, and MTA3 is concurrently downregulated during breast cancer progression, leading to an elevated expression of ZEB2, which, in turn, represses the expression of G9A and MTA3 through the recruitment of G9A/NuRD(MTA1).

INTRODUCTION

GATA3 is the most highly expressed transcription factor in the mammary epithelium and is expressed exclusively in the luminal epithelial cell population where it not only specifies, but also maintains luminal epithelial cell differentiation (Asselin-Labat et al., 2007; Kouros-Mehr et al., 2006). However, the expression of GATA3 is progressively lost during luminal breast cancer progression, and low GATA3 expression is strongly correlated with higher histologic grade, poor differentiation, positive lymph nodes, estrogen receptor negative and progesterone receptor negative status, and HER2/neu overexpression, all indicators of poor prognosis (Kouros-Mehr et al., 2008; Yoon et al., 2010). In addition, mutations in GATA3 that diminish or abolish its DNA-binding ability are commonly found in human breast cancers (Usary et al., 2004), and GATA3 was reported to be one of three genes mutated in >10% of all breast cancers (The Cancer Genome Atlas Network, 2012). However, how lost expression/loss-of-function of GATA3 contributes to the dissemination and metastasis of breast cancer is still poorly understood.

G9A/Eu-HMTase2/KMT1C is a histone lysine methyltransferase that biochemically catalyzes mono- and di-methylation of H3K9 (H3K9me1 and H3K9me2) in euchromatin and is functionally linked to transcription repression (Collins et al., 2008; Feldman et al., 2006; Tachibana et al., 2002). Interestingly, although gene ablation of *G9a* in mice results in embryonic lethality, G9a$^{-/-}$ embryonic stem cells do not show overt growth abnormalities in culture conditions, but exhibit severe differentiation defects, suggesting a role for G9A in cell differentiation and

Significance

Our study suggests that a reciprocal feedback regulatory loop between GATA3/G9A/NuRD(MTA3) and ZEB2/G9A/NuRD(MTA1) is implemented in mammary epithelium to dictate the epithelial cell fate and to govern the dynamics of the epithelial cell plasticity in the mammary gland, whose dysfunction contributes to the metastasis of breast cancer. Our data provide a mechanistic link of the loss-of-function of GATA3 to breast cancer progression and a molecular mechanism underlying the opposing action of MTA1 and MTA3 in breast cancer progression. Our results add to the understanding of the complexity of the hierarchical regulatory network of EMT and support the pursuit of GATA3, ZEB2, G9A, and MTA1/MTA3 as the potential prognostic indicators or/and therapeutic targets of breast cancer.

lineage commitment (Tachibana et al., 2002). Importantly, G9A has also been implicated in the development and progression of a variety of human cancers including hepatocellular, colon, prostate, lung, and bladder carcinomas (Shankar et al., 2013).

MTA (metastasis tumor antigen) family proteins, MTA1, MTA2, and MTA3, are the integral component of the Mi-2/nucleosome remodeling and deacetylase (NuRD) complex that is primarily implicated in transcription repression (Wang et al., 2009; Zhang et al., 1998). It is believed that the members of MTA family do not co-localize in the same NuRD complex and do not functionally substitute for each other (Denslow and Wade, 2007; Fujita et al., 2003; Yao and Yang, 2003). Intriguingly, although all MTA1, MTA2, and MTA3 have been implicated in cancer progression and metastasis (Denslow and Wade, 2007; Kumar, 2003; Manavathi and Kumar, 2007), it was noted that MTA1 and MTA3 exhibit opposite patterns of expression during breast cancer: similar to GATA3, MTA3 is highly expressed in epithelial cells, and its expression is progressively lost during breast cancer progression, whereas MTA1 expression progressively increases during the process (Zhang et al., 2006). Functionally, MTA1 promotes breast tumor progression, whereas MTA3 has an opposing role by inhibiting epithelial-to-mesenchymal transition (EMT) (Fujita et al., 2003). However, the molecular mechanism underlying the opposite functionality of MTA1 and MTA3 in breast cancer development is still not understood.

EMT programs are coordinated by a set of pleiotropic transcription factors including SNAIL, TWIST, and zinc-finger E-box-binding (ZEB) transcription factors. The two vertebrate ZEB transcription factors, ZEB1 and ZEB2, can either repress or activate transcription (Peinado et al., 2007). It has been reported that ZEB2 is expressed in breast cancer cells and its level of expression is negatively correlated with that of the epithelial marker E-cadherin (Lee et al., 2014). However, how ZEB2 coordinates with other EMT regulators and contributes to breast cancer progression are largely unexplored.

In this study, we addressed the issue of how loss of function of GATA3 contributes to the development of breast cancer. We explored the molecular mechanism underlying the opposing action of MTA1 and MTA3 and investigated the functional interplay between GATA3 and ZEB2, two master regulators of EMT, in breast cancer progression.

RESULTS

GATA3 Is Physically Associated with G9A and the NuRD(MTA3) Complex

To understand how the loss of function of GATA3 contributes to the breast cancer metastasis, we first employed affinity purification and mass spectrometry to interrogate GATA3 interactome in vivo. In these experiments, FLAG-tagged GATA3 (FLAG-GATA3) was stably expressed in human breast adenocarcinoma cell line MCF-7. Whole cell extracts were prepared and subjected to affinity purification using an anti-FLAG affinity gel. Mass spectrometric analysis indicates that GATA3 was co-purified with MTA3, HDAC1, HDAC2, RbAp46, RbAp48, all components of the NuRD complex, as well as with G9A, a H3K9 methyltransferase (Figure 1A). The presence of G9A and the NuRD subunits in the GATA3 interactome was confirmed by western blotting analysis of the column-bound proteins with antibodies against the corresponding proteins (Figure 1A, right). The detailed result of the mass spectrometric analysis is provided in Table S1.

To further support the in vivo interaction between GATA3, G9A, and the NuRD complex, total proteins from MCF-7 cells were extracted and co-immunoprecipitation experiments were performed with antibodies detecting the endogenous proteins. Immunoprecipitation (IP) with antibodies against GATA3 followed by immunoblotting (IB) with antibodies against G9A, Mi-2, LSD1, HDAC1, HDAC2, RbAp46/48, MBD3, MTA1, MTA2, or MTA3 demonstrated that all the tested proteins, except for MTA1 and MTA2, were efficiently co-immunoprecipitated with GATA3 (Figure 1B). Reciprocally, IP with antibodies against G9A or components of the NuRD(MTA1/2/3) complex followed by IB with antibodies against GATA3 also showed that GATA3 was efficiently co-immunoprecipitated by G9A and all the components of the NuRD complex except for MTA1 and MTA2 (Figure 1B, right). These results suggest that GATA3 is physically associated with G9A and MTA3-, but not MTA1- or MTA2-, associated NuRD complex in vivo. Corroborating with this, IP using equal amounts of MCF-7 cellular extracts with antibodies against MTA1 or MTA3, followed by immunoblotting with antibodies against GATA3, G9A, MTA1, MTA2, MTA3, Mi-2, HDAC1, or MBD3 indicate that while G9A was co-immunoprecipitated with both MTA1 and MTA3, GATA3 was only co-immunoprecipitated with MTA3 (Figure 1C).

To verify the presence of a GATA3/G9A/NuRD(MTA3) complex in vivo, MCF-7 nuclear proteins were fractionated by fast protein liquid chromatography (FPLC) with Superose 6 columns and a high salt extraction and size exclusion approach. We found that the native GATA3 from MCF-7 cell nuclear extracts was eluted with an apparent molecular mass much greater than that of the monomeric protein; GATA3 immunoreactivity was detected in chromatographic fractions from the Superose 6 column with a relative symmetric peak centered between ~669 and ~2,000 kDa (Figure 1D). Significantly, the elution pattern of GATA3 largely overlapped with that of G9A and the NuRD complex proteins including Mi-2, MTA proteins, HDAC2, and RbAp46/48. Furthermore, western blotting of FLAG-GATA3 affinity eluate from FPLC after Superose 6 gel filtration revealed that GATA3 was only co-immunoprecipitated with MTA3 (Figure 1E). These observations support the existence of the GATA3/G9A/NuRD(MTA3) complex in vivo.

To substantiate the observation that GATA3 is specifically associated with the MTA3-consitituted NuRD complex, affinity purification and mass spectrometry were utilized again to analyze G9A-, MTA1-, and MTA3-associated proteins in vivo. Notably, G9A was co-purified with GATA3, Mi-2, LSD1, HDAC1, HDAC2, RbAp46, RbAp48, MBD3, and all three MTA family members, MTA1, MTA2, and MTA3 (Figure 1F). The presence of these proteins in the G9A-containing complex was confirmed by western blotting analysis of the column-bound proteins with antibodies against the corresponding proteins (Figure 1F, right). Interestingly, however, although G9A was co-purified with both MTA1 and MTA3, GATA3 was only found in the MTA3-containing protein complex (Figure 1G). These results were confirmed by co-IP experiments in MCF-7 cells and

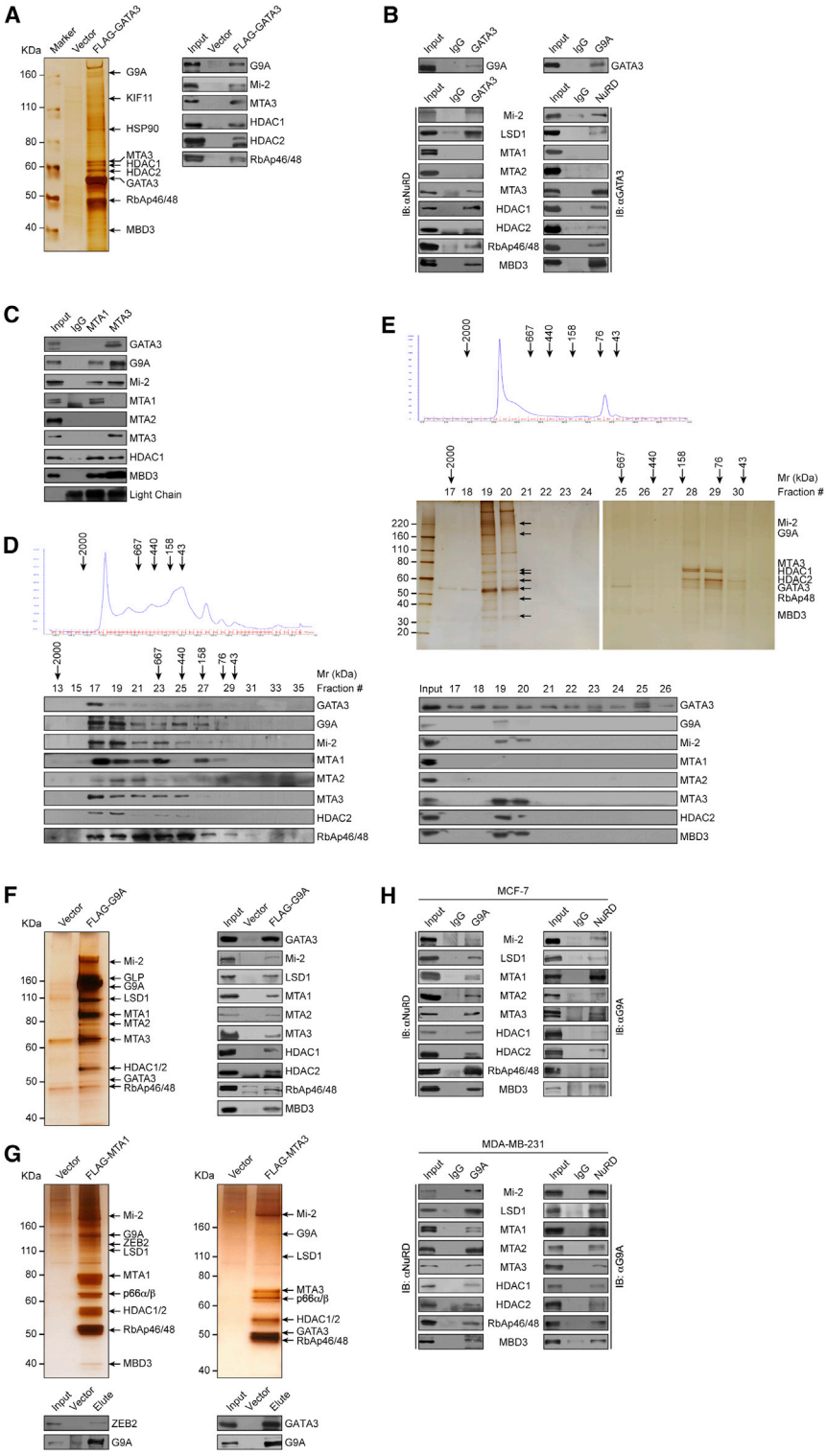

Figure 1. GATA3 Interacts with G9A and the MTA3-Associated NuRD Complex

(A) Cellular extracts from MCF-7 cells stably expressing FLAG (control) or FLAG-GATA3 were immunopurified with anti-FLAG affinity columns and eluted with FLAG peptide. The eluates were resolved by SDS-PAGE and silver-stained. The protein bands were retrieved and analyzed by mass spectrometry. Column-bound proteins were analyzed by western blotting using antibodies against the indicated proteins.

(B) Whole cell lysates from MCF-7 cells were prepared and co-IP was performed with antibodies against the indicated proteins. Immunocomplexes were then IB using antibodies against the indicated proteins.

(C) Equal amounts of MCF-7 cellular extracts were immunoprecipitated with antibodies against MTA1 or MTA3 followed by IB with antibodies against the indicated proteins.

(D) Nuclear extracts of MCF-7 cells were fractionated on Superose 6 size exclusion columns. Chromatographic elution profiles and IB analysis of the chromatographic fractions are shown. Equal volume from each fraction was analyzed and the elution positions of calibration proteins with known molecular masses (kDa) are indicated.

(E) Silver staining and western blotting of the GATA3-containing complex fractionated by Superose 6 gel filtration.

(F and G) Immunopurification and mass spectrometric analysis of G9A-, MTA1-, or MTA3-containing proteins in MCF-7 cells.

(H) Whole cell lysates from MCF-7 cells or MDA-MB-231 cells were immunoprecipitated with antibodies against the indicated proteins. Immunocomplexes were then IB using antibodies against the indicated proteins.

See also Tables S1, S2, S3, and S4.

Molecular Interaction between GATA3, G9A, and the NuRD(MTA3) Complex

To further support the physical association between GATA3, G9A, and the NuRD(MTA3) complex and to gain insights into the molecular details involved in the interaction of these proteins, glutathione S-transferase (GST) pull-down experiments were then performed by incubation of GST-fused GATA3 with in vitro transcribed/translated individual components of the NuRD complex including G9A, LSD1, MTA1, MTA2, MTA3, HDAC1, HDAC2, RbAp46, RbAp48, and MBD3. We showed that GATA3 interacts directly with G9A and MTA3, but not with the other components of the NuRD complex tested (Figure 2A). Reciprocal GST pull-down experiments with GST-fused G9A, LSD1, MTA1, MTA2, MTA3, HDAC1, HDAC2, RbAp46, RbAp48, or MBD3 and in vitro transcribed/translated GATA3 yielded similar results (Figure 2B). In addition, MDA-MB-231 cells (Figure 1H). Altogether, the above experiments indicate that GATA3 specifically interacts with G9A and the MTA3-associated NuRD in vivo. The detailed result of the mass spectrometric analysis is provided in Tables S2, S3, and S4.

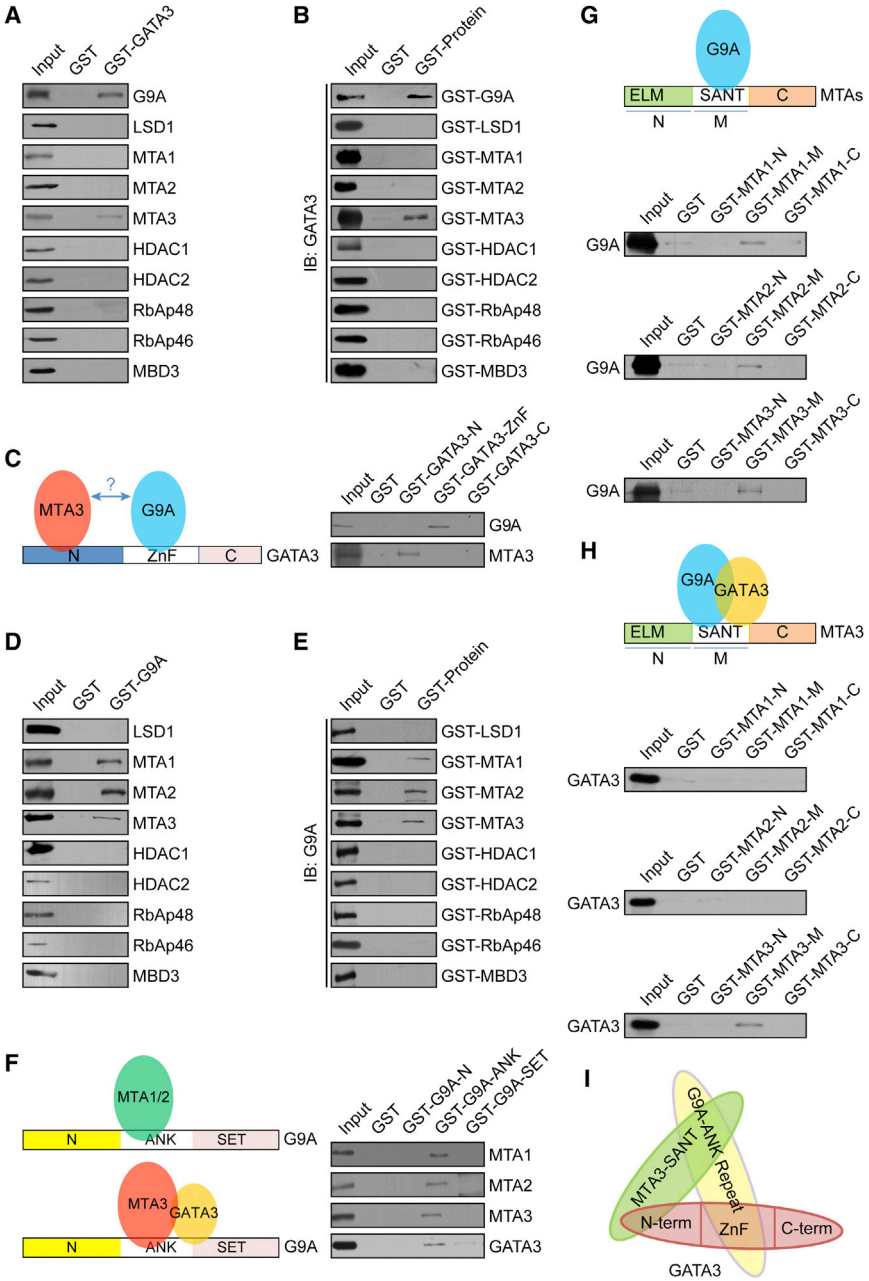

Figure 2. Molecular Interaction between GATA3, G9A, and the NuRD Complex

(A–H) GST pull-down assays with GST-fused proteins and in vitro transcribed/translated proteins as indicated.

(I) Schematic diagram depicting the molecular interaction between GATA3, G9A, and MTA3 is shown.

GST pull-down assays with GST-fused N-terminal fragment (1–222 amino acid [aa], GATA3-N), the zinc finger domain (222–333 aa, GATA3-ZnF), or the C-terminal fragment (333–444 aa, GATA3-C) of GATA3 and in vitro transcribed/translated G9A or MTA3 indicated that the N-terminal region of GATA3 is responsible for its interaction with MTA3 and the zinc finger region of GATA3 is responsible for its interaction with G9A (Figure 2C).

Analogously, GST pull-down assays with GST-fused G9A and in vitro transcribed/translated components of the NuRD complexes revealed that G9A is able to interact with all three MTA proteins, MTA1, MTA2, and MTA3 (Figure 2D), consistent with the results from affinity purification and co-IP described above. Reciprocal GST pull-down experiments with GST-fused NuRD components and in vitro transcribed/translated G9A yielded similar results (Figure 2E). Likewise, GST pull-down assays with GST-fused G9A N-terminal fragment (1–266 aa, G9A-N), the ANK repeat domain (266–744 aa, G9A-ANK), or the SET domain (676–1211 aa, G9A-SET) and in vitro transcribed/translated GATA3 or MTA1/2/3 demonstrated that the ANK repeat domain of G9A is responsible for its interaction with MTAs and GATA3 (Figure 2F). Moreover, GST pull-down assays with GST-fused N-terminal fragment (MTA-N), middle region (MTA-M), or C-terminal fragment (MTA-C) of MTA1/2/3 and in vitro transcribed/translated G9A or GATA3 suggest that the Swi3-Ada2-N-CoR-TFIIIB (SANT) domain of MTAs is responsible for the interaction of MTA1/2/3 with G9A and of MTA3 with GATA3 (Figures 2G and 2H). Together, these results not only provided further support of the specific interaction between GATA3, G9A, and the NuRD(MTA3) complex, but also delineated the molecular detail involved in the formation of the GATA3/G9A/NuRD(MTA3) complex, as schematically summarized (Figure 2I).

Identification of Genome-wide Transcription Targets for the GATA3/G9A/NuRD(MTA3) Complex

As mentioned earlier, GATA3 is a transcription factor acting to either activate or repress gene transcription. However, both G9A and the NuRD(MTA3) complex are mainly implicated in gene transcription repression. The association of GATA3 with G9A and the NuRD(MTA3) complex suggest that the GATA3-nucleated chromatin modifying complex GATA3/G9A/NuRD(MTA3) constitutes a repression program functioning to inhibit gene transcription. In order to explore the functional significance of the physical association between GATA3, G9A, and the NuRD(MTA3) complex, we analyzed the genome-wide transcriptional targets of the GATA3/G9A/NuRD(MTA3) complex by chromatin IP-based deep sequencing (ChIP-seq). In these experiments, ChIP experiments were performed first in MCF-7 cells with antibodies against GATA3, G9A, or MTA3. Following ChIP, GATA3-, G9A-, and MTA3-associated DNAs were

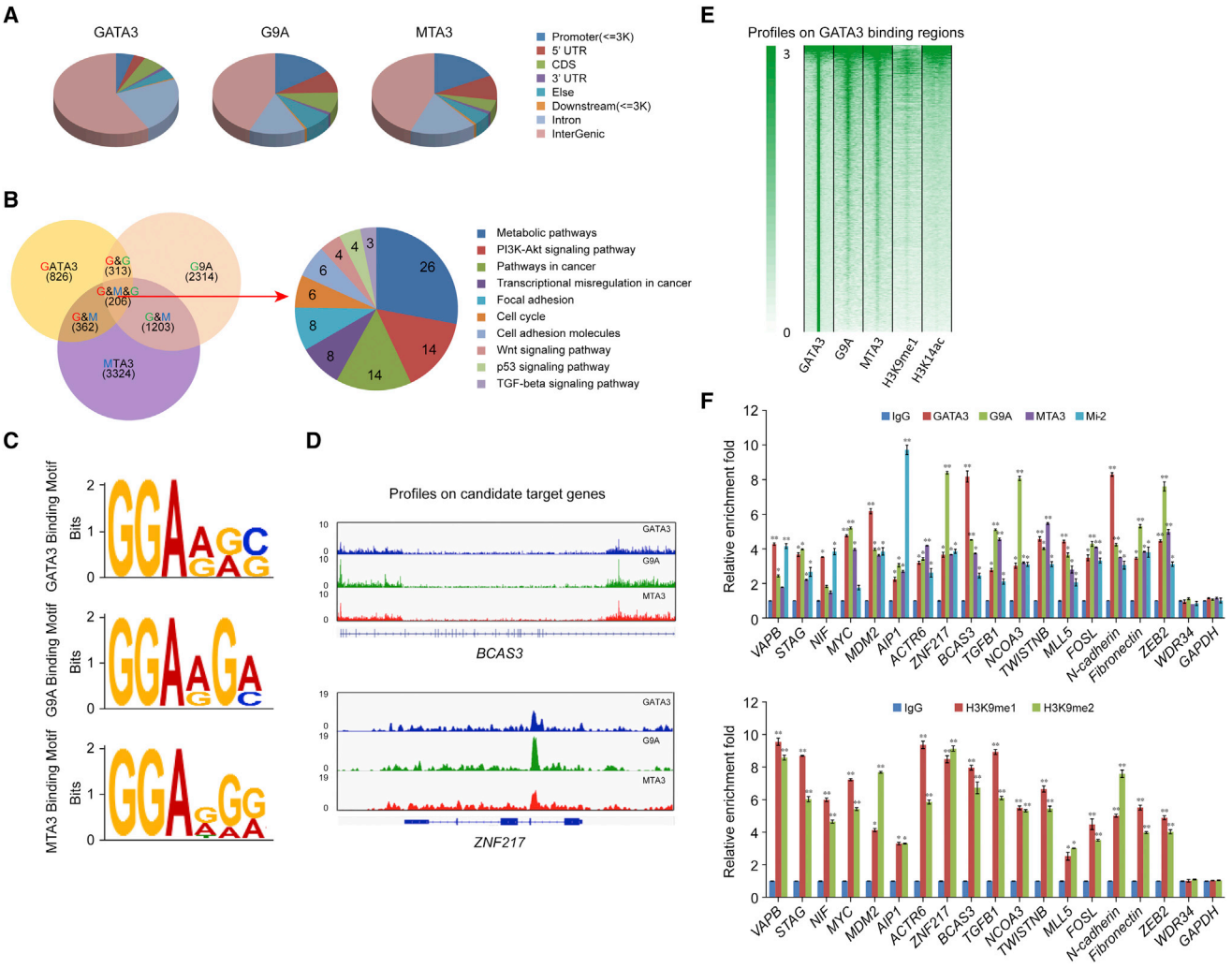

Figure 3. Genome-wide Transcription Target Analysis for the GATA3/G9A/NuRD(MTA3) Complex

(A) Genomic distribution of GATA3, G9A, and MTA3 determined by ChIP-seq analysis.

(B) The Venn diagram of overlapping promoters bound by GATA3, G9A, and MTA3 in MCF-7 cells (left). The clustering of the 206 overlapping target genes of GATA3/G9A/MTA3 into functional groups is shown (right). The detailed results of the ChIP-seq experiments are provided in the Supplemental Experimental Procedures.

(C) GATA3-, G9A-, and MTA3-bound motifs were analyzed using MEME suite.

(D) The binding of GATA3, G9A, and MTA3 on representative target genes, *ZNF217* and *BCAS3*. The chromosome number and position of the peak bound by each of the proteins are shown.

(E) ChIP-seq density heatmaps of G9A, MTA3, H3K9me1, and H3K14ac on GATA3 binding sites.

(F) Verification of the ChIP-seq results by qChIP analysis of the indicated genes in MCF-7 cells. Results are represented as fold change over control with glyceraldehyde 3-phosphate dehydrogenase (GAPDH) as a negative control. Error bars represent mean ± SD for three independent experiments (*$p < 0.05$, **$p < 0.01$, and two-tailed unpaired t test).

See also Table S5.

amplified using non-biased conditions, labeled, and then sequenced. Using HiSeq2000 and with a p value cutoff of 10^{-5}, we identified 9,934 GATA3-specific binding peaks, 14,480 G9A-specific binding sites, and 18,750 MTA3-specific binding sequences (Figure 3A) (GEO accession number: GSE67206). The data from GATA3, G9A, and MTA3 groups were then analyzed for overlapping DNA sequences/gene promoters, and these promoters were considered to be the targets of the GATA3/G9A/NuRD(MTA3) complex. These experiments identified a total of 206 different promoters targeted by GATA3, G9A, and MTA3. The corresponding genes to these promoters were then classified into various cellular signaling pathways using Molecule Annotation System software with a p value cut off of 10^{-3}. These signaling pathways include metabolic, P13K-Akt, focal adhesion, cell cycle, cell adhesion, Wnt, p53, and TGF-β pathways that are critically involved in cell growth, survival, migration, and invasion (Figure 3B). Significantly, we found that GATA3, G9A, and MTA3 had similar binding motifs (Figure 3C), genomic distributions, and peak locations on the proximal promoter of the target genes such as *BCAS3* and *ZNF217*

(Figure 3D), supporting the notion that GATA3, G9A, and MTA3 physically interact and are functionally linked.

We also analyzed the genomic landscapes of the GATA3/G9A/NuRD(MTA3) complex as well as the enzymatic activities associated with this complex by intercrossing GATA3/G9A/MTA3 ChIP-seq data with published ChIP-seq results for various histone modifications in MCF-7 cells (Wu et al., 2013). Comparing the characteristic enrichment of G9A, MTA3, H3K9me1, and H3K14 acetylation (H3K14ac) at GATA3 binding sites versus randomly selected genomic control regions revealed that G9A, MTA3, and H3K9me1 were significantly enriched in regions surrounding the GATA3 genomic binding sites, whereas H3K14ac exhibited little difference between GATA3 binding sites and the non-specific regions (Figure 3E). Detailed results of the ChIP-seq experiments are provided in Table S5 and deposited in GEO data sets.

Quantitative ChIP (qChIP) analysis in MCF-7 cells using specific antibodies against GATA3, G9A, MTA3, or Mi-2 on selected genes including *VAPB*, *STAG*, *NIF*, *MYC*, *MDM2*, *AIP1*, *ACTR6*, *ZNF217*, *BCAS3*, *TGFB1*, *NCOA3*, *TWISTNB*, *MLL5*, *FOSL*, *CDH2* (*N-cadherin*), *FN1* (*Fibronectin*), and *ZEB2* that represent each of the classified pathways showed a strong enrichment of GATA3, G9A, MTA3, and Mi-2 on the promoters of these genes, validating the ChIP-seq results (Figure 3F). In addition, qChIP analysis with specific antibodies against H3K9me1 and H3K9me2, two catalytic products of G9A, showed that the target promoters were indeed marked with H3K9me1 and H3K9me2 (Figure 3F), further supporting the occupancy of these promoters by G9A.

The Formation of the GATA3/G9A/NuRD(MTA3) Repression Complex on Transcriptional Targets

In order to support the notion that GATA3, G9A, and MTA3 occupy the target promoters in the context of the GATA3/G9A/NuRD(MTA3) complex, MCF-7 cell clones with GATA3, G9A, or MTA3 stably depleted were generated by lentivirus-delivered short hairpin RNA (shRNA) (Figures 4A and S1). qChIP experiments indicated that while depletion of either GATA3, G9A, or MTA3 resulted in a marked reduction of the recruitment of the corresponding proteins at the promoters of the target genes, depletion of G9A or MTA3 resulted in only marginal or no effect on the recruitment of GATA3 (Figure 4B). However, when GATA3 was depleted, the recruitment of G9A and MTA3, as well as Mi-2, to the target promoters was dramatically reduced (Figure 4B), although the expression of G9A and MTA3 was not affected by GATA3 knockdown (Figure 4A). Consistently, the levels of H3K9me1 and H3K9me2 were markedly decreased at all the tested target promoters upon knockdown of either G9A or GATA3, while the level of pan-H3 acetylation (H3Ac) was significantly increased when either MTA3 or GATA3 was depleted (Figure 4C). Interestingly, although G9A and MTA3 had little effect on each other's chromatin binding (Figure 4B), their catalytic activities appeared to be interdependent (Figure 4C). These results point to a scenario in which the chromatin modifying enzymes G9A and NuRD(MTA3) are recruited on target gene promoters by GATA3, supporting the existence of GATA3, G9A, and the NuRD(MTA3) in the same protein complex on target gene promoters and the functional coordination between these chromatin modifiers.

To further support the proposition that GATA3 nucleates G9A and NuRD(MTA3) to form one protein complex at target promoters, sequential ChIP or ChIP/Re-ChIP experiments were performed on four representative target genes, *ZEB2*, *BCAS3*, *TGFB1*, and *N-cadherin*. In these experiments, soluble chromatins were first immunoprecipitated with antibodies against GATA3, G9A, or MTA3. The immunoprecipitates were subsequently re-immunoprecipitated with appropriate antibodies. The results showed that, in precipitates, the *ZEB2*, *BCAS3*, *TGFB1*, and *N-cadherin* promoters that were immunoprecipitated with antibodies against GATA3 could be re-immunoprecipitated with antibodies against G9A or MTA3 (Figure 4D). Similar results were obtained when initial ChIP was done with antibodies against G9A or MTA3 (Figure 4D). These results support the argument that GATA3, G9A, and the NuRD(MTA3) complex occupy the *ZEB2*, *BCAS3*, *TGFB1*, and *N-cadherin* promoters as one protein complex. In agreement with this, depletion of GATA3, G9A, or MTA3 in MCF-7 cells led to increased expression of ZEB2, BCAS3, TGFB1, and N-cadherin (Figure 4E, left).

The GATA3/G9A/NuRD(MTA3) Complex Inhibits EMT and the Invasive Potential of Breast Cancer Cells In Vitro and Suppresses Breast Cancer Metastasis In Vivo

As stated above, our genome-wide analysis indicates that the GATA3/G9A/NuRD(MTA3) targets several cellular signaling pathways that are critically involved in cell migration and invasion. In order to further support the physical interaction and to explore the functional connection between GATA3, G9A, and the NuRD(MTA3) complex, we next investigated the role of the GATA3/G9A/NuRD(MTA3) complex in invasion and metastasis of breast cancer. To this end, gain of function and loss of function of GATA3, G9A, or MTA3 experiments were performed, and the expression of epithelial/mesenchymal markers was analyzed and the morphological alterations were examined in MCF-7 cells. We found that overexpression of either GATA3, G9A, or MTA3 resulted in induction, at both mRNA and protein levels, of epithelial protein markers including E-cadherin, α-catenin, and γ-catenin and reduction of mesenchymal markers including N-cadherin, fibronectin, and vimentin, and co-overexpression of G9A and MTA3 led to more pronounced changes in the expression of these markers (Figure 5A). Consistently, depletion of GATA3, G9A, or MTA3 individually or in combination resulted in the reduction of epithelial markers and induction of mesenchymal markers (Figures 5B and S2A). Moreover, experiments with GATA3 depletion indicated that the induction or depression of these markers by overexpression of G9A and MTA3 is, at least partially, dependent of GATA3 (Figure 5C). Morphologically, while control cells maintained organized cell-cell adhesion and cell polarity, GATA3-, G9A-, or MTA3-deficient cells exhibited loss of cell-cell contacts; cells became scattered and their cobble stone-like appearance was replaced by a spindle-like, fibroblastic morphology, indicative of characteristic morphological changes of EMT (Figure S2B). Consistently, immunofluorescent microscopic analysis showed a reduced or lost membrane staining of epithelial markers E-cadherin and α-catenin in GATA3-, G9A-, or MTA3-depleted MCF-7 cells, while the staining of the mesenchymal markers N-cadherin and fibronectin exhibited a reverse trend (Figure S2B).

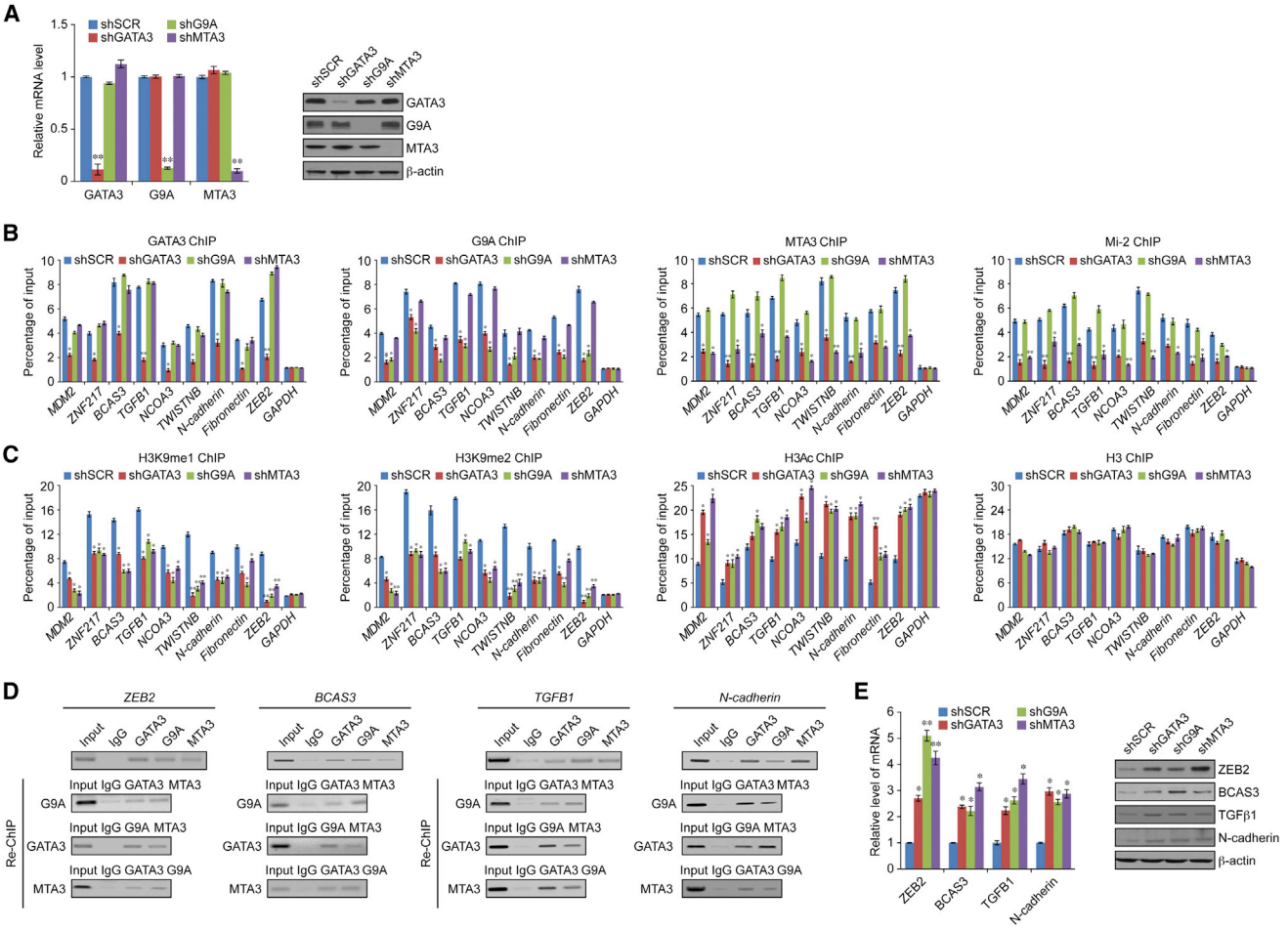

Figure 4. The Formation of the GATA3/G9A/NuRD(MTA3) Complex on Transcription Targets

(A) MCF-7 cells were infected with lentivirus carrying control shRNA (shSCR) or shRNAs targeting GATA3, G9A, or MTA3. The knockdown efficiencies of GATA3, G9A, and MTA3 were verified by real-time RT PCR and western blotting.

(B and C) MCF-7 cells were infected with lentiviruses carrying the indicated shRNAs. qChIP analysis of the selected promoters was performed using antibodies against GATA3, G9A, MTA3, or Mi-2 (B) or against H3K9me1, H3K9me2, or H3Ac (C). H3 was detected as an internal control. Results are represented as fold change over control with GAPDH as a negative control.

(D) ChIP and Re-ChIP experiments in MCF-7 cells with the indicated antibodies.

(E) Real-time RT PCR and western blotting analyses of the expression of ZEB2, BCAS3, TGFB1, and N-cadherin in MCF-7 cells infected with lentiviruses carrying the indicated shRNAs. Error bars represent mean ± SD for three independent experiments (*$p < 0.05$, **$p < 0.01$, and two-tailed unpaired t test).

See also Figure S1.

We then investigated the roles of GATA3, G9A, and MTA3 in cellular behavior of breast cancer cells in vitro using transwell invasion assays. As shown in Figure 5D, knockdown of GATA3, G9A, or MTA3 led to an increase in the invasive potential of MCF-7 cells, whereas overexpression of either GATA3, G9A, or MTA3 resulted in a decrease in the invasive potential of MDA-MB-231 cells. Significantly, in agreement with the functional link between GATA3/G9A/MTA3 and ZEB2 described earlier, the positive effect of GATA3/G9A/MTA3 knockdown on the invasive potential of non-invasive MCF-7 cells could be offset by transfection of cells with ZEB2 shRNA, while the inhibitory effect on the invasive potential of the invasive MDA-MB-231 cells associated with GATA3, G9A, or MTA3 overexpression could be offset by ectopic expression of ZEB2 (Figures 5D, S2C, and S2D). In addition, the inhibitory effect of GATA3 overexpression on invasiveness was probably achieved through a concerted action by the G9A/MTA3/NuRD complex, as the effect of GATA3 overexpression was diminished when either G9A or MTA3 was concomitantly knocked down in MDA-MB-231 cells (Figures 5D and S2D). Taken together, these results support a critical role for the GATA3/G9A/NuRD(MTA3) complex in the regulation of EMT and invasion.

We then investigated the role of the GATA3/G9A/NuRD(MTA3) complex in breast cancer metastasis in vivo. For this purpose, MDA-MB-231 cells that were engineered to stably express firefly luciferase (MDA-MB-231-Luc-D3H2LN, Xenogen) were co-infected with lentiviruses carrying GATA3 and lentiviruses carrying G9A shRNA or MTA3 shRNA. These cells were then orthotopically implanted onto nude mice or intravenously injected into immunocompromised severe combined immunodeficiency

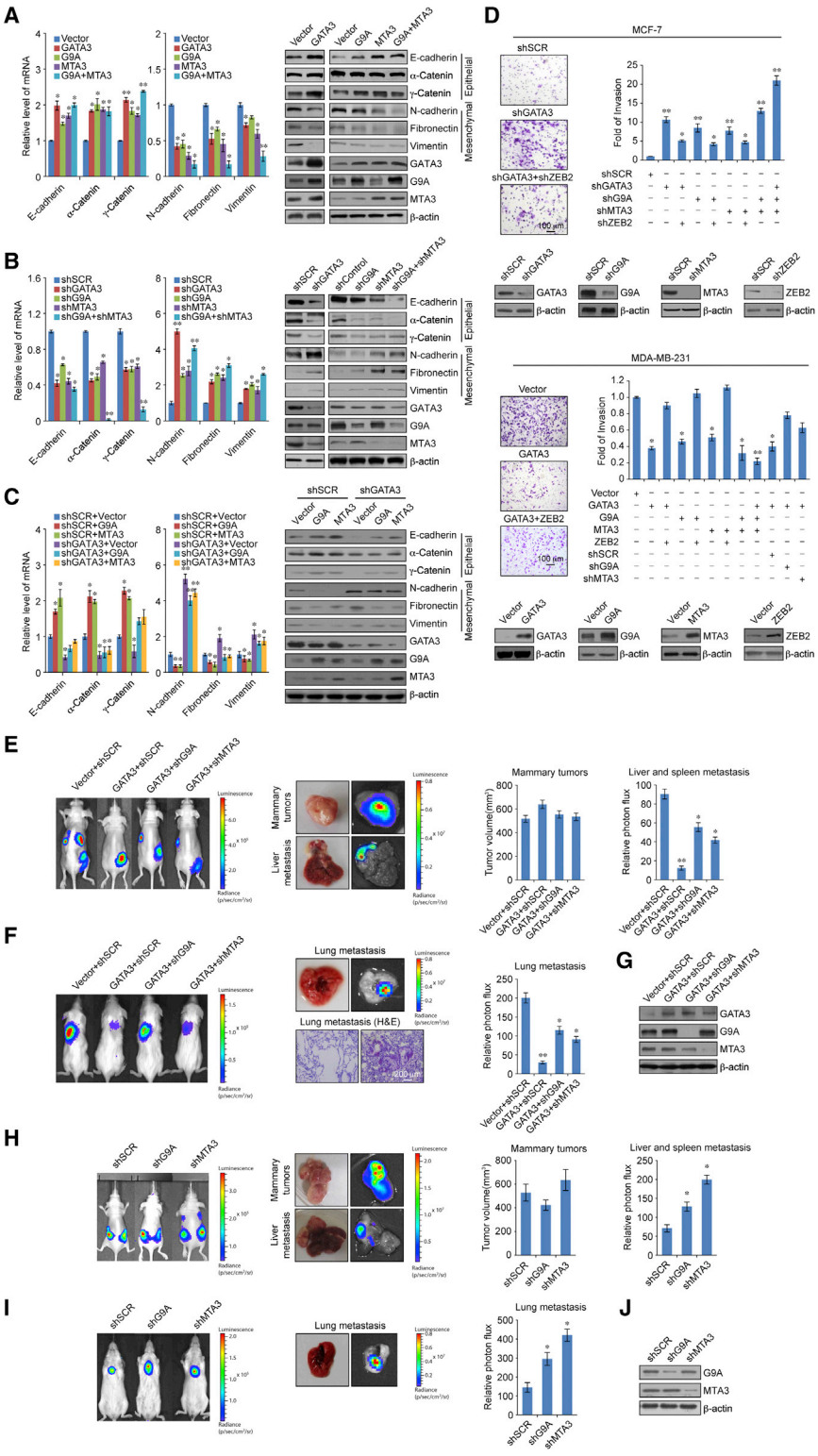

Figure 5. The GATA3/G9A/NuRD(MTA3) Complex Inhibits the Invasive Potential of Breast Cancer Cells In Vitro and Suppresses Breast Cancer Metastasis In Vivo

(A–C) The expression of the indicated epithelial or mesenchymal markers was measured by real-time RT PCR (left) or western blotting (right) in MCF-7 cells overexpressing GATA3, G9A, or/and MTA3 (A), MCF-7 cells with GATA3, G9A, or/and MTA3 depleted (B), or MCF-7 cells co-transfected with shGATA3 and the expression plasmids for G9A or MTA3 (C).

(D) Non-invasive MCF-7 cells and invasive MDA-MB-231 cells were transfected with the indicated specific shRNAs or/and expression constructs for cell invasion assays. The invaded cells were stained and counted. The images represent one field under microscopy in each group. The efficiency of protein knockdown or overexpression was verified by western blotting.

(E and H) MDA-MB-231-Luc-D3H2LN cells infected with lentiviruses carrying GATA3, GATA3, and shRNA against G9A (GATA3+shG9A), or GATA3 and shRNA against MTA3 (GATA3+shMTA3) (E), shRNA against G9A or MTA3 (H) were inoculated orthotopically into the abdominal mammary fat pad of 6-week-old female nude mice (n = 8). Primary tumors and metastases were quantified using bioluminescence imaging after 7 weeks of initial implantation. Representative in vivo bioluminescent images are shown (left), and tumor specimens were examined by in vitro bioluminescent measurement (middle).

(F and I) The above-described MDA-MB-231-Luc-D3H2LN cells were injected intravenously through the tail vein of 6-week-old female SCID mice (n = 8). Lung metastasis was quantified using bioluminescence imaging after 6 weeks. Representative in vivo bioluminescent images are shown (left). Lung cancer specimens were examined by in vitro bioluminescent measurement and the sections from normal (untreated) or GATA3+shG9A-treated mice were stained with hematoxylin and eosin (H&E) (middle). Error bars indicate mean ± SD (*p < 0.05, **p < 0.01, and two-tailed paired t test).

(G and J) The protein expression in MDA-MB-231-Luc-D3H2LN cells was confirmed by western blotting.

See also Figure S2.

(SCID) mice for the measurements of spontaneous metastasis or seeding lung metastasis, respectively. Specifically, MDA-MB-231-Luc-D3H2LN cells were either implanted onto the abdominal mammary fat pad (n = 8) of 6-week-old female nude mice or injected into the lateral tail vein (n = 8) of 6-week-old female SCID mice. The growth/dissemination of tumors was monitored weekly by bioluminescence imaging with the IVIS imaging system (Xenogen). Tumor metastasis was measured by quantitative bioluminescence imaging after 7 weeks for the orthotopically implanted groups. For the intravenous injection groups, the quantitative bioluminescence imaging was performed at 6 weeks after injection. A metastatic event was defined as any detectable luciferase signal above background and away from the primary tumor site. The results showed that, in the orthotopically implanted groups, although GATA3 overexpression alone did not affect the

growth of the primary MDA-MB-231-Luc-D3H2LN tumors, it resulted in a significant reduction in liver metastasis of the tumors (Figure 5E). Remarkably, although no effect on the growth of primary MDA-MB-231-Luc-D3H2LN tumors, depletion of either G9A or MTA3 abrogated GATA3 overexpression-associated suppression of the metastasis (Figure 5E). Similarly, in the intravenous injection groups, GATA3 overexpression led to a dramatic decrease in lung metastasis of the MDA-MB-231-Luc-D3H2LN tumors and the suppressive effect of GATA3 overexpression on lung metastasis was, at least partially, abolished when either G9A or MTA3 was knocked down (Figure 5F). The metastases to the lungs were verified by bioluminescence imaging and histological staining (Figure 5F) and the efficiency of overexpression or knockdown was verified by western blotting (Figure 5G). We also showed that knockdown of either G9A or MTA3 promoted breast cancer metastasis (Figures 5H–5J). Collectively, these experiments indicate that GATA3 suppresses breast cancer metastasis in a G9A- and MTA3-dependent manner, supporting a role for the GATA3/G9A/NuRD(MTA3) complex in controlling the metastasis of breast cancer in vivo.

Reciprocal Feedback Regulation by GATA3/G9A/NuRD(MTA3) and ZEB2/G9A/NuRD(MTA1) in Controlling Breast Cancer Progression

In order to gain further support of the role of the GATA3/G9A/NuRD(MTA3) complex in breast cancer progression and to extend our observations to a clinicopathologically relevant setting, we collected 115 breast carcinoma samples from human breast cancer patients and performed tissue microarrays by immunohistochemical staining to examine the expression of GATA3, G9A, and MTA3 in breast cancer samples (Figure 6A). Strikingly, we found that the expression of GATA3, G9A, and MTA3 is concurrently downregulated in breast cancer samples and the levels of their expression are negatively correlated with the histological grades of the tumors (Figure 6B). In addition, consistent with our observation that ZEB2 is a downstream target of the GATA3/G9A/NuRD(MTA3) complex, the expression of ZEB2 was found to be upregulated in these breast cancer samples and the level of its expression is positively correlated with the histological grades of breast cancers (Figure 6B). When the relative expression level of ZEB2 was plotted against that of GATA3/G9A/MTA3 in 30 samples of grades I–II breast carcinomas, statistically significant negative correlations were observed (Figure 6C).

The concurrent downregulation of GATA3, G9A, and MTA3 in breast carcinomas is intriguing. Nevertheless, this scenario fits well to our working model that GATA3, G9A, and MTA3 are functionally connected through formation of the GATA3/G9A/NuRD(MTA3) complex. The question is how the expression of GATA3, G9A, and MTA3 is all downregulated or concurrently lost during breast cancer progression. Based on the reports that ZEB2 is a transcription repressor and also a powerful regulator of EMT (Gregory et al., 2008; Lamouille et al., 2014; Peinado et al., 2007) and on our observations that ZEB2 is a downstream target of the GATA3/G9A/NuRD(MTA3) complex, and is upregulated in breast carcinomas, and that its expression is inversely correlated with that of GATA3, G9A, or MTA3, it is possible that elevated expression of ZEB2 is functionally linked to the concurrent downregulation of GATA3, G9A, and MTA3. There are two lines of evidence that support the hypothesis that ZEB2 transcriptionally represses the expression of G9A and MTA3, but not GATA3, in breast cancer cells: first, knockdown of ZEB2 expression by its specific shRNA in MCF-7, MDA-MB-231, T-47D, and MDA-MB-453 cells led to a derepression of G9A and MTA3, but not GATA3 (Figure 6D); and second, ChIP experiments detected that ZEB2, but not ZEB1, SNAI1 (Snail), SNAI2 (Slug), TWIST1 (Twist) or TWIST2, indeed occupies the promoters of G9A and MTA3 (Figure 6E).

In order to gain mechanistic insights into ZEB2-mediated repression of G9A and MTA3, affinity purification and mass spectrometry were utilized again to identify ZEB2 interactome in MDA-MB-231 cells. The results indicated that ZEB2 is associated with a number of proteins including Mi-2, MTA1, MTA2, HDAC1, HDAC2, RbAp46, RbAp48, and MBD3, all components of the NuRD complexes, as well as G9A, in vivo (Figure 7A). The presence of these proteins in ZEB2-associated complexes was confirmed by western blotting analysis of the eluate with specific antibodies against these proteins (Figure 7A, right). The detailed result of the mass spectrometric analysis is provided in Table S6. FPLC assays revealed that ZEB2 immunoreactivity was detected in MDA-MB-231 cell nuclear extracts in chromatographic fractions from the Superose 6 column with a relative symmetric peak centered between ~669 and ~2,000 kDa and the elution pattern of ZEB2 largely overlapped with that of G9A and of the NuRD complex proteins including MTA proteins, RbAp46/48, and MBD3 (Figure 7B). Furthermore, western blotting of FLAG-ZEB2 affinity eluate from FPLC after Superose 6 gel filtration revealed that ZEB2 was only co-immunoprecipitated with MTA1/2 (Figure 7C). These observations support the existence of the ZEB2/G9A/NuRD(MTA1/2) complex in vivo. Furthermore, IP with anti-ZEB2 followed by IB with antibodies against G9A, Mi-2, MTA1, MTA2, HDAC1, HDAC2, RbAp46/48, or MBD3 indicated that all these proteins were efficiently co-immunoprecipitated with ZEB2 (Figure 7D). Reciprocal co-IP with antibodies against G9A, Mi-2, MTA1, MTA2, HDAC1, HDAC2, RbAp46/48, or MBD3 followed by IB with anti-ZEB2 yielded similar results (Figure 7D). Notably, both affinity purification and co-IP detected no physical association between ZEB2 and MTA3. In addition, GST pull-down with GST-fused LSD1, G9A, MTA1, MTA2, MTA3, HDAC1, HDAC2, RbAp46, RbAp48, or MBD3 and in vitro transcribed/translated ZEB2 revealed that ZEB2 interacts with G9A as well as with MTA1 and MTA2, but not with MTA3 and other components of the NuRD complex tested (Figure 7E). These experiments indicate that ZEB2 is physically associated with G9A/NuRD(MTA1/2) through directly binding to G9A and MTA1/MTA2.

To further delineate the molecular mechanism underlying ZEB2-mediated transcription repression of G9A and MTA3, MTA1 or MTA2 was overexpressed in MCF-7 cells or depleted in MDA-MB-231 cells and the expression of G9A and MTA3 was measured by western blotting. The results of the experiments indicated that overexpression of MTA1, but not MTA2, was associated with a reduction of G9A and MTA3 in MCF-7 cells (Figure 7F). Likewise, knockdown of the expression of MTA1, but not MTA2, resulted in an elevated expression of G9A and MTA3 in MDA-MB-231 cells (Figure 7F). These experiments suggest that ZEB2 represses the expression of G9A and

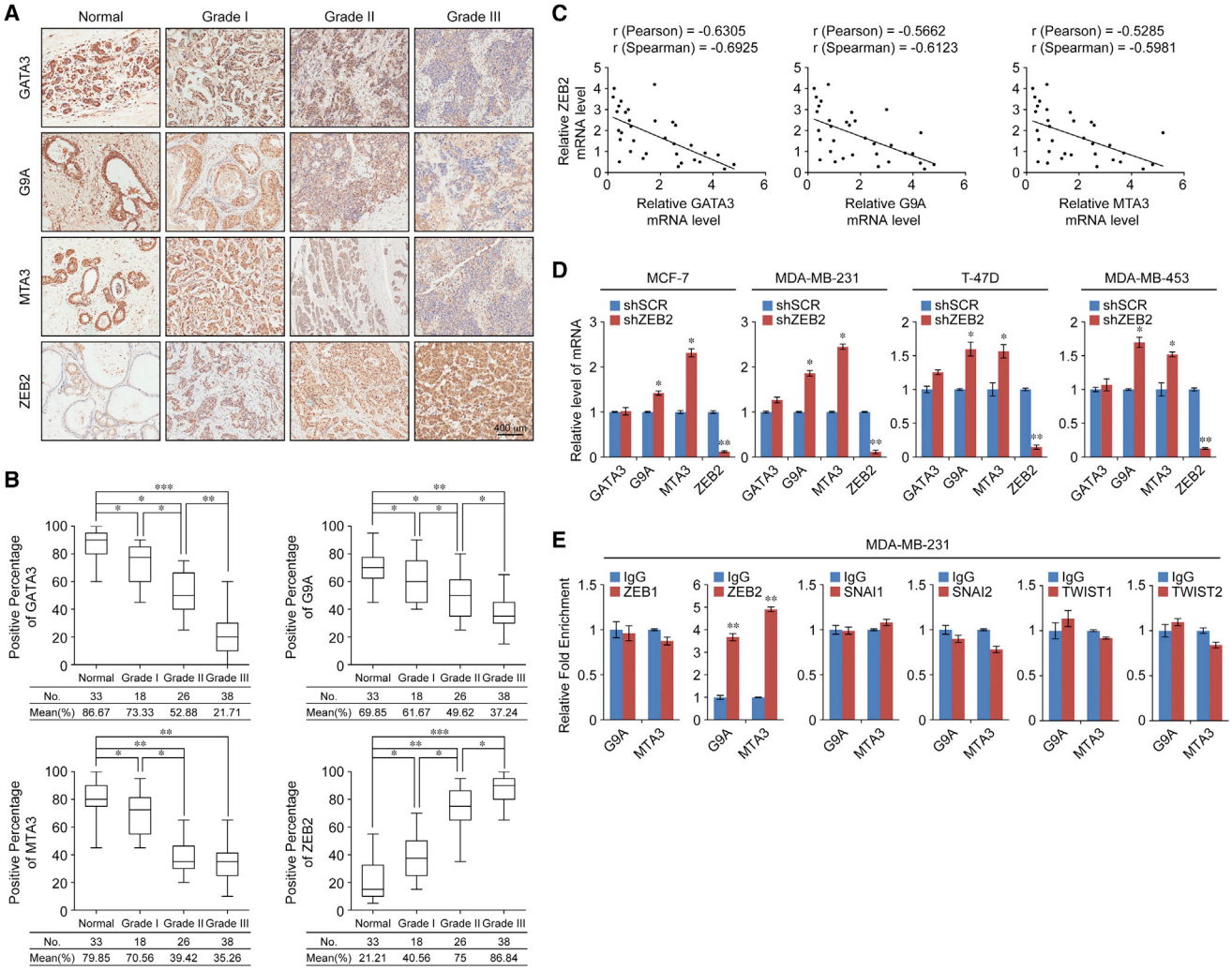

Figure 6. Reciprocal Feedback Regulation by GATA3/G9A/NuRD(MTA3) and ZEB2 G9A/NuRD(MTA1) in Controlling Breast Cancer Metastasis

(A) Immunohistochemical staining of GATA3, G9A, MTA3, and ZEB2 in normal breast tissues and breast carcinomas (histological grades I, II, and III).

(B) The positively stained nuclei (%) in grouped samples were analyzed by two-tailed unpaired t test (*$p < 0.05$, **$p < 0.01$, and ***$p < 0.001$).

(C) The expression of GATA3, G9A, MTA3, or ZEB2 mRNAs was analyzed by real-time RT PCR in 30 paired breast carcinoma samples of grades I–II. The relative level of ZEB2 was plotted against that of GATA3, G9A, or MTA3 with GAPDH as the reference.

(D) MCF-7, MDA-MB-231, T-47D, and MDA-MB-453 cells were treated with control shRNA or ZEB2 shRNA, and the expression of the mRNA of GATA3, G9A, and MTA3 was measured by real-time RT PCR.

(E) qChIP assays were performed using the indicated antibodies in MDA-MB-231 cells. Error bars represent mean ± SD for three independent experiments.

MTA3 through formation of a ZEB2/G9A/NuRD(MTA1) complex. To test this hypothesis, ChIP and Re-ChIP assays were then performed on the promoters of G9A and MTA3. The results showed that ZEB2, G9A, MTA1, as well as Mi-2, occupy the promoters of G9A and MTA3 in one protein complex (Figure 7G). In vitro transwell invasion assays indicated that overexpression of ZEB2 in non-invasive MCF-7 cells was associated with an increased invasiveness of the cells, an effect that could be offset by simultaneous knockdown of MTA1 or overexpression of either G9A or MTA3, whereas knockdown of ZEB2 in invasive MDA-MB-231 cells resulted in a decreased invasiveness of the cells, an effect that could be mimicked by knockdown of either G9A or MTA3 (Figures 7H and S3). Collectively, these results support the argument that ZEB2 represses the expression of G9A and MTA3 through recruitment of G9A and the NuRD(MTA1) complex. Additionally, based on their low expression in corresponding cell lines (Figure 7I), ZEB2 or GATA3 was overexpressed in MCF-7 or MDA-MB-231 cells, respectively. Equal amounts of cellular extracts were immunoprecipitated with antibodies against ZEB2 or GATA3 followed by IB with antibodies against Mi-2, HDAC1, MBD3, G9A, MTA1, or MTA3 (Figure 7I). These experiments showed that ZEB2 and GATA3 competitively interacted with G9A and NuRD proteins except for MTA molecules. If our interpretation of these results is correct, it means that a reciprocal feedback regulatory loop exists between GATA3- and ZEB2-nucleated

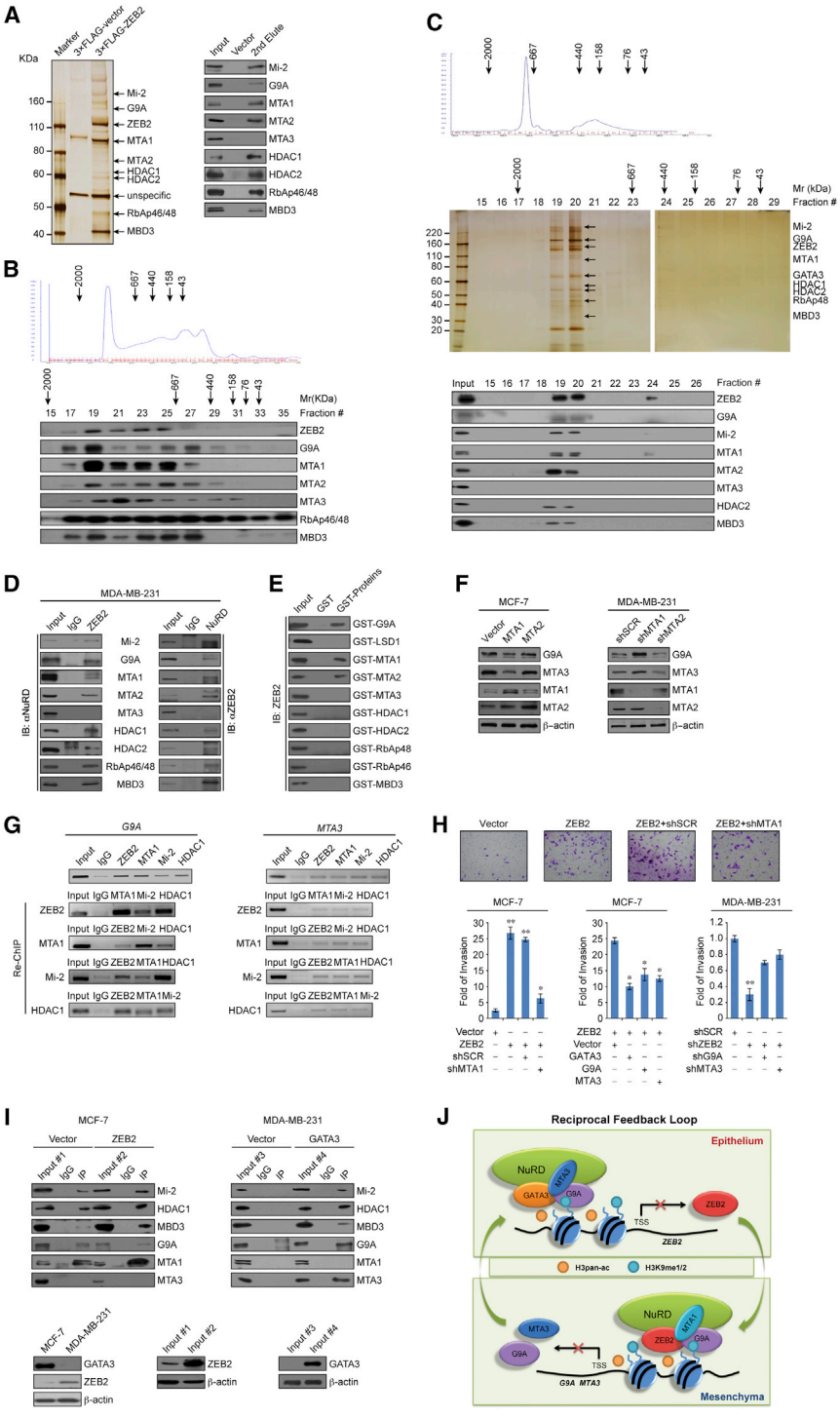

Figure 7. Transcription Repression of G9A and MTA3 by the ZEB2/G9A/NuRD(MTA1) Complex

(A) Immunopurification and mass spectrometric analysis of ZEB2-associated proteins in MDA-MB-231 cells. Column-bound proteins were detected by western blotting using antibodies against the indicated proteins (right). (B) Co-fractionation of ZEB2 complex in MDA-MB-231 cells by FPLC.

(C) Silver staining and western blotting of ZEB2-containing complex fractionated by Superose 6 gel filtration.

(D) Co-IP assays in MDA-MB-231 cells.

(E) GST pull-down assays with the indicated GST-fused proteins and in vitro transcribed/translated ZEB2.

(F) MTA1 or MTA2 was overexpressed in MCF-7 cells or knocked down in MDA-MB-231 cells, the expression of G9A and MTA3 in these cells was detected by western blotting.

(G) ChIP and Re-ChIP experiments in MCF-7 cells with the indicated antibodies.

(H) Non-invasive MCF-7 cells and invasive MDA-MB-231 cells were transfected with the indicated shRNAs or/and expression constructs for cell invasion assays. Error bars indicate mean ± SD for a representative experiment performed in triplicate (*$p < 0.05$, **$p < 0.01$, and two-tailed unpaired t test).

(I) ZEB2 was overexpressed in MCF-7 and GATA3 was overexpressed in MDA-MB-231 cells. Equal amounts of MCF-7 or MDA-MB-231 cellular extracts were co-immunoprecipitated with antibodies against ZEB2 or GATA3, followed by IB with the indicated antibodies.

(J) The proposed reciprocal feedback regulatory loop between GATA3/G9A/NuRD(MTA3) and ZEB2/G9A/NuRD(MTA1).

See also Figure S3 and Table S6.

repression programs in controlling the EMT and metastasis of breast cancer (Figure 7J).

Finally, to further extend our observations to a clinicopathologically relevant context, we analyzed the expression of GATA3 and its correlation with clinical behaviors of breast cancer patients. Kaplan-Meier survival analysis of GATA3/G9A with another online tool (http://kmplot.com/analysis/) showed that both higher GATA3 expression ($p = 0.0065$) and higher G9A expression ($p = 0.047$) were associated with a better overall survival of breast cancer patients (n = 1,005), when the influence of systemic treatment, endocrine therapy, and chemotherapy was excluded (Figures 8A and S4). In addition, although similar clinical data for MTA3 is not available, Kaplan-Meier survival analysis of the published data sets (Ivshina et al., 2006) demonstrated that higher ZEB2 expression is associated with a worse overall survival of the patients ($p = 0.04681$), and further stratification of patient groups based on the inverse expression of GATA3/ZEB2 improved the predictive capability of ZEB2 ($p = 0.012739$) (Figure 8B), supporting ZEB2 being another significant predictor of survival. Moreover, analysis of three published clinical data sets (GSE1456, GSE2034, and GSE4922) revealed statistically significant negative correlations of expression between G9A and ZEB2 (Figure 8C), supporting our overall argument, although G9A was reported to repress E-cadherin and promote breast cancer metastasis (Dong et al., 2012).

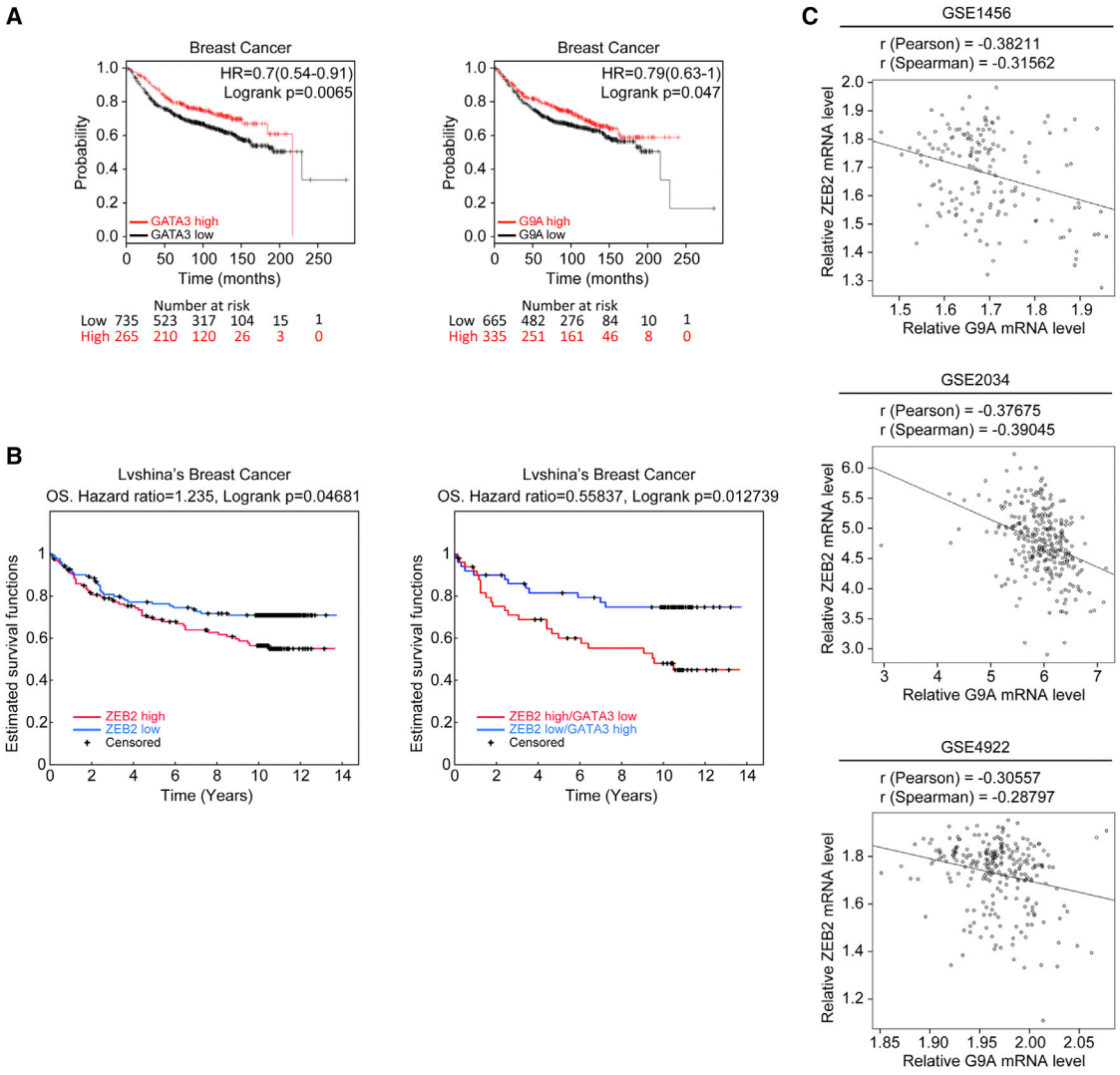

Figure 8. Clinicopothological Significance of GATA3/G9A/ZEB2 in Breast Cancer

(A) Kaplan-Meier survival analysis for the relationship between survival time and GATA3/G9A signature in breast cancer using the online tool (http://kmplot.com/analysis/).

(B) Kaplan-Meier survival analysis of the published data sets (Ivhsina; GSE4922) for the relationship between survival time and ZEB2/GATA3 signature in breast cancer.

(C) Analysis of public data sets (GSE1456, GSE2034, and GSE4922) for the expression of ZEB2, GATA3, and G9A. The relative level of ZEB2 was plotted against that of G9A.

See also Figure S4.

DISCUSSION

We report in this study that in breast cancer cells, GATA3 acts as a transcriptional repressor that recruits chromatin remodeling G9A/NuRD(MTA3) complex to inhibit the expression of a set of genes including *ZEB2*, *TGFB1*, *MDM2*, *ZNF217*, and *BCAS3* that are known to be critically involved in EMT, a hallmark of cancer metastasis (Hanahan and Weinberg, 2011). Interestingly, we showed that the GATA3/G9A/NuRD(MTA3) complex also targets the repression of a group of genes including *N-cadherin* and *Fibronecitin* that represent the molecular markers of EMT. Apparently, through a physical interaction, transcriptional regulators GATA3, G9A, and the NuRD(MTA3) act in a concerted manner and cooperated fashion to formulate a transcription repression program to regulate the mammary epithelial plasticity by controlling the hierarchical molecular network of EMT.

$G9a^{-/-}$ embryonic stem cells show severe differentiation defects (Tachibana et al., 2002), and, remarkably, mutant mice with catalytically inactive G9A also have an embryonic lethal phenotype similar to that of G9A knockout mice (Dodge et al., 2004), suggesting that G9A-mediated H3K9 methylation is important for its biological function. G9A catalyzes mono- and di-methylation of H3K9 in euchromatin (Collins et al., 2008; Feldman et al., 2006; Shinkai and Tachibana, 2011; Tachibana et al., 2002), prominent histone modifications that demarcate transcription repression (Martin and Zhang, 2005). Our observation

that G9A is recruited to chromatin by GATA3 and represses gene expression is consistent with these notions. In addition, we showed that G9A directly interacts with all three members of the MTA family and constitutes a facultative component of the NuRD complex. It is believed that the NuRD complex contains several subunits whose pattern of expression is heterogeneous in various cell and tissue types, and it is proposed that subunit heterogeneity confers these complexes with additional regulatory capacity and with unique functional properties (Bowen et al., 2004; Denslow and Wade, 2007). In this regard, it is interesting to note that previously we reported that the H3K4 demethylases LSD1 (Wang et al., 2009) and JARID1B (Li et al., 2011) are associated with the NuRD complex, expanding the enzymatic repertoire of the NuRD complex to include, in addition to the ATPase and deacetylase, demethylase activity. Yet, our current identification of the physical association and functional link between G9A and the NuRD complex activity extends the enzymatic arsenal of the NuRD complex to include a histone methyltransferase. It is possible that G9A and LSD1 act in a coordinated fashion in the context of the NuRD complex to simultaneously or sequentially methylate H3K9 and demethylate H3K4, two histone modifications that are well linked to transcription repression. In any event, it appears that Mi-2, MTAs, and HDAC1/2 represent the compulsory components of the NuRD complex and constitute the command center or headquarters of the NuRD complex, which, through enlisting additional transcriptional co-regulators, largely catalytic enzymes, to fulfill different missions.

We showed that NuRD/(MTA3) is recruited by GATA3 and NuRD(MTA1) is recruited by ZEB2. Since GATA3 controls the epithelial traits and the ZEB2 dictates the mesenchymal features in mammary epithelium, our current study not only provides a molecular basis for the opposing action of MTA3 and MTA1 in breast cancer progression, but also adds to the understanding of the molecular interplays involved in the sophisticated regulatory network of EMT, although it remains to be delineated the interplays among different regulatory pathways including GATA3, ZEB2, Snail, Twist, and others that control EMT processes. Moreover, it is possible that differential usage of MTA species is tissue specific. For example, GATA3 has been previously reported to physically interact with MTA2 in Th2 cells (Hwang et al., 2010).

We showed that the GATA3/G9A/NuRD(MTA3) complex is a potent suppressor of breast cancer metastasis through targeting the promoters of an array of genes that represent several important cellular signaling pathways regulating cell migration and invasion. A number of the genes, including *ZEB2*, *ZFXH1B*, *SIP1*, *MDM2*, *ZNF217*, and *BCAS3* have been implicated in the development and progression of a variety of human malignancies, and suppression of breast cancer invasion and metastasis by GATA3 has also been reported by others (Chou et al., 2013; Yan et al., 2010). It is probably too early to call the GATA3/G9A/NuRD(MTA3) complex a master suppressor of EMT and metastasis. Nevertheless, our observation that the GATA3/G9A/NuRD(MTA3) complex transcriptionally represses all the above genes positions the GATA3/G9A/NuRD(MTA3) complex upstream of these genes and places GATA3/G9A/MTA3 at the node of the hierarchical regulatory network of EMT, providing mechanistic insights into the functional similarity and interplays of above-described genes in the development and progression of breast cancer. Of note, we showed that overexpression of GATA3 did not affect the growth of primary tumors, whereas studies by others reported that this condition did affect the growth of primary tumors (Chou et al., 2013; Yan et al., 2010). The reason behind this discrepancy needs further investigation.

Yet, ZEB2 is at another epicenter and represents another node of the hierarchical regulatory network of EMT. However, contrary to GATA3, ZEB2 is a powerful promoter of EMT. Acting as a transcription repressor and through downregulation of E-cadherin and microRNA miR-200 family and upregulation of mesenchymal markers (Gregory et al., 2008; Peinado et al., 2007), ZEB2 positively influences cellular signaling pathways including TGFβ and Wnt pathway to promotes EMT and metastasis. Thus, the transcription repression of ZEB2 by the GATA3/G9A/NuRD(MTA3) complex is of particular significance. In effect, GATA3, through the aid of G9A/NuRD(MTA3), inhibits the expression of the mesenchymal promoter ZEB2 and maintains the luminal cell fate in mammary epithelium. Upon loss of function of GATA3 due to lost expression or mutations, which occurs frequently in breast cancer (Kouros-Mehr et al., 2008; Mehra et al., 2005; The Cancer Genome Atlas Network, 2012; Usary et al., 2004; Yoon et al., 2010), the expression of ZEB2 is derepressed, and elevated ZEB2 promotes EMT and metastasis. Although this is a logic scenario to explain how loss of function of GATA3 contributes to the progression of breast cancer, it is apparently not the whole story. We found that, surprisingly, the expression of GATA3, G9A, and MTA3 is concurrently downregulated in advanced breast carcinomas and we demonstrated that ZEB2 is the culprit. We showed that ZEB2, through recruitment of G9A and the MTA1-constituted NuRD complex, represses the expression of G9A and MTA3. Apparently, a reciprocal feedback regulatory loop exists in which loss of function of GATA3 in breast cancer leads to an elevated expression of ZEB2, which, in turn, further downregulates G9A and MTA3 to maintain its high level of expression, promotes EMT, and, eventually, leads to the metastasis of breast cancer. In this loop, although G9A acting to repress itself initially appears to be enigmatic, it nonetheless might be an integral component of the mechanism and represent a rate-limiting factor in this system.

In summary, our results suggest that a reciprocal feedback regulatory loop between GATA3/G9A/NuRD(MTA3) and ZEB2/G9A/NuRD(MTA1) is implemented in mammary epithelium to dictate the epithelial cell fate and to govern the dynamics of the epithelial cell plasticity in the mammary gland, whose dysfunction affects the fate of mammary epithelial cells and contributes to the metastasis of breast cancer. Our data provide a mechanistic link of the loss of function of GATA3 to breast cancer progression and a molecular mechanism underlying the opposing action of MTA1 and MTA3 in the development and progression of breast cancer. Our results add to the understanding of the complexity of the hierarchical regulatory network of EMT and support the pursuit of GATA3, ZEB2, G9A, and MTA1/MTA3 as the potential prognostic indicators or/and therapeutic targets of breast cancer.

EXPERIMENTAL PROCEDURES

For a detailed description of all methods, see the Supplemental Experimental Procedures.

In Vivo Metastasis

MDA-MB-231 cells that had been transfected to stably express firefly luciferase (Xenogen) were infected with lentiviruses carrying empty vector, GATA3 expression construct, control shRNA, shG9A, or shMTA3. These cells were inoculated into the left abdominal mammary fat pad (3∼4 × 10^6 cells) of 6-week-old female nude mice or injected into the lateral tail vein (1∼3 × 10^6 cells) of 6-week-old female SCID mice. For bioluminescence imaging, mice were injected with 200 mg/g of D-luciferin in PBS abdominally. At 15 min after injection, mice were anesthetized and bioluminescence was imaged with a charge-coupled device camera (IVIS; Xenogen). Bioluminescence images were obtained with a 15 cm field of view, binning (resolution) factor of eight, 1/f stop, open filter, and an imaging time of 30 s to 2 min. Bioluminescence from relative optical intensity was defined manually. Photon flux was normalized to background, which was defined from a relative optical intensity drawn over a mouse not given an injection of luciferin. Animal handling and procedures were approved by the Tianjin Medical University Institutional Animal Care.

Tissue Specimens

Normal mammary tissues, specimen with pathological grades I, II, and III breast cancers, were procured from surgical specimens from patients with breast cancer for which complete information on clinical tumor size and metastatic status was available. All human tissue was collected using protocols approved by the Ethics Committee of the Peking University Health Science Center and informed consent was obtained from all patients.

Statistical Analysis

Results were reported as mean ± SD unless otherwise noted. SPSS V.17.0 was used for statistical analysis. Comparisons between cancer and adjacent normal tissue were performed using paired samples t test based on a bi-directional hypothesis for continuous variables. Breast tumor data sets were downloaded from http://www.ncbi.nlm.nih.gov/geo (Ivhsina; GSE4922, Wang; GSE2034, Ivshina; GSE4922). The TCGA data were from http://bioinformatics.mdanderson.org/main/TCPA:Overview. Data for Kaplan-Meier survival analysis were from http://kmplot.com/analysis/index.php?p=service&cancer=breast.

ACCESSION NUMBER

ChIP-seq data are deposited at the Gene Expression Omnibus database (http://www.ncbi.nlm.nih.gov/geo/) with an accession number GSE67206.

SUPPLEMENTAL INFORMATION

Supplemental Information includes Supplemental Experimental Procedures, four figures, and six tables and can be found with this article online at http://dx.doi.org/10.1016/j.ccell.2015.04.011.

ACKNOWLEDGMENTS

We thank Dr. Su Wang (Tongji University, China) for assistance in ChIP-seq analysis. This work was supported by grants (91219201 and 81130048 to Y.S. and 81322032 to Y.W.) from the National Natural Science Foundation of China and grants (973 Program: 2011CB504204 to Y.S. and 2014CB542004 to J.L.) from the Ministry of Science and Technology of China.

Received: October 13, 2014
Revised: February 17, 2015
Accepted: April 17, 2015
Published: May 28, 2015

REFERENCES

Asselin-Labat, M.L., Sutherland, K.D., Barker, H., Thomas, R., Shackleton, M., Forrest, N.C., Hartley, L., Robb, L., Grosveld, F.G., van der Wees, J., et al. (2007). Gata-3 is an essential regulator of mammary-gland morphogenesis and luminal-cell differentiation. Nat. Cell Biol. *9*, 201–209.

Bowen, N.J., Fujita, N., Kajita, M., and Wade, P.A. (2004). Mi-2/NuRD: multiple complexes for many purposes. Biochim. Biophys. Acta *1677*, 52–57.

Chou, J., Lin, J.H., Brenot, A., Kim, J.W., Provot, S., and Werb, Z. (2013). GATA3 suppresses metastasis and modulates the tumour microenvironment by regulating microRNA-29b expression. Nat. Cell Biol. *15*, 201–213.

Collins, R.E., Northrop, J.P., Horton, J.R., Lee, D.Y., Zhang, X., Stallcup, M.R., and Cheng, X. (2008). The ankyrin repeats of G9a and GLP histone methyltransferases are mono- and dimethyllysine binding modules. Nat. Struct. Mol. Biol. *15*, 245–250.

Denslow, S.A., and Wade, P.A. (2007). The human Mi-2/NuRD complex and gene regulation. Oncogene *26*, 5433–5438.

Dodge, J.E., Kang, Y.K., Beppu, H., Lei, H., and Li, E. (2004). Histone H3-K9 methyltransferase ESET is essential for early development. Mol. Cell. Biol. *24*, 2478–2486.

Dong, C., Wu, Y., Yao, J., Wang, Y., Yu, Y., Rychahou, P.G., Evers, B.M., and Zhou, B.P. (2012). G9a interacts with Snail and is critical for Snail-mediated E-cadherin repression in human breast cancer. J. Clin. Invest. *122*, 1469–1486.

Feldman, N., Gerson, A., Fang, J., Li, E., Zhang, Y., Shinkai, Y., Cedar, H., and Bergman, Y. (2006). G9a-mediated irreversible epigenetic inactivation of Oct-3/4 during early embryogenesis. Nat. Cell Biol. *8*, 188–194.

Fujita, N., Jaye, D.L., Kajita, M., Geigerman, C., Moreno, C.S., and Wade, P.A. (2003). MTA3, a Mi-2/NuRD complex subunit, regulates an invasive growth pathway in breast cancer. Cell *113*, 207–219.

Gregory, P.A., Bert, A.G., Paterson, E.L., Barry, S.C., Tsykin, A., Farshid, G., Vadas, M.A., Khew-Goodall, Y., and Goodall, G.J. (2008). The miR-200 family and miR-205 regulate epithelial to mesenchymal transition by targeting ZEB1 and SIP1. Nat. Cell Biol. *10*, 593–601.

Hanahan, D., and Weinberg, R.A. (2011). Hallmarks of cancer: the next generation. Cell *144*, 646–674.

Hwang, S.S., Lee, S., Lee, W., and Lee, G.R. (2010). GATA-binding protein-3 regulates T helper type 2 cytokine and ifng loci through interaction with metastasis-associated protein 2. Immunology *131*, 50–58.

Ivshina, A.V., George, J., Senko, O., Mow, B., Putti, T.C., Smeds, J., Lindahl, T., Pawitan, Y., Hall, P., Nordgren, H., et al. (2006). Genetic reclassification of histologic grade delineates new clinical subtypes of breast cancer. Cancer Res. *66*, 10292–10301.

Kouros-Mehr, H., Slorach, E.M., Sternlicht, M.D., and Werb, Z. (2006). GATA-3 maintains the differentiation of the luminal cell fate in the mammary gland. Cell *127*, 1041–1055.

Kouros-Mehr, H., Bechis, S.K., Slorach, E.M., Littlepage, L.E., Egeblad, M., Ewald, A.J., Pai, S.Y., Ho, I.C., and Werb, Z. (2008). GATA-3 links tumor differentiation and dissemination in a luminal breast cancer model. Cancer Cell *13*, 141–152.

Kumar, R. (2003). Another tie that binds the MTA family to breast cancer. Cell *113*, 142–143.

Lamouille, S., Xu, J., and Derynck, R. (2014). Molecular mechanisms of epithelial-mesenchymal transition. Nat. Rev. Mol. Cell Biol. *15*, 178–196.

Lee, J.Y., Park, M.K., Park, J.H., Lee, H.J., Shin, D.H., Kang, Y., Lee, C.H., and Kong, G. (2014). Loss of the polycomb protein Mel-18 enhances the epithelial-mesenchymal transition by ZEB1 and ZEB2 expression through the downregulation of miR-205 in breast cancer. Oncogene *33*, 1325–1335.

Li, Q., Shi, L., Gui, B., Yu, W., Wang, J., Zhang, D., Han, X., Yao, Z., and Shang, Y. (2011). Binding of the JmjC demethylase JARID1B to LSD1/NuRD suppresses angiogenesis and metastasis in breast cancer cells by repressing chemokine CCL14. Cancer Res. *71*, 6899–6908.

Manavathi, B., and Kumar, R. (2007). Metastasis tumor antigens, an emerging family of multifaceted master coregulators. J. Biol. Chem. *282*, 1529–1533.

Martin, C., and Zhang, Y. (2005). The diverse functions of histone lysine methylation. Nat. Rev. Mol. Cell Biol. *6*, 838–849.

Mehra, R., Varambally, S., Ding, L., Shen, R., Sabel, M.S., Ghosh, D., Chinnaiyan, A.M., and Kleer, C.G. (2005). Identification of GATA3 as a breast cancer prognostic marker by global gene expression meta-analysis. Cancer Res. *65*, 11259–11264.

Peinado, H., Olmeda, D., and Cano, A. (2007). Snail, Zeb and bHLH factors in tumour progression: an alliance against the epithelial phenotype? Nat. Rev. Cancer *7*, 415–428.

Shankar, S.R., Bahirvani, A.G., Rao, V.K., Bharathy, N., Ow, J.R., and Taneja, R. (2013). G9a, a multipotent regulator of gene expression. Epigenetics *8*, 16–22.

Shinkai, Y., and Tachibana, M. (2011). H3K9 methyltransferase G9a and the related molecule GLP. Genes Dev. *25*, 781–788.

Tachibana, M., Sugimoto, K., Nozaki, M., Ueda, J., Ohta, T., Ohki, M., Fukuda, M., Takeda, N., Niida, H., Kato, H., and Shinkai, Y. (2002). G9a histone methyltransferase plays a dominant role in euchromatic histone H3 lysine 9 methylation and is essential for early embryogenesis. Genes Dev. *16*, 1779–1791.

The Cancer Genome Atlas Network (2012). Comprehensive molecular portraits of human breast tumours. Nature *490*, 61–70.

Usary, J., Llaca, V., Karaca, G., Presswala, S., Karaca, M., He, X., Langerød, A., Kåresen, R., Oh, D.S., Dressler, L.G., et al. (2004). Mutation of GATA3 in human breast tumors. Oncogene *23*, 7669–7678.

Wang, Y., Zhang, H., Chen, Y., Sun, Y., Yang, F., Yu, W., Liang, J., Sun, L., Yang, X., Shi, L., et al. (2009). LSD1 is a subunit of the NuRD complex and targets the metastasis programs in breast cancer. Cell *138*, 660–672.

Wu, X., Johansen, J.V., and Helin, K. (2013). Fbxl10/Kdm2b recruits polycomb repressive complex 1 to CpG islands and regulates H2A ubiquitylation. Mol. Cell *49*, 1134–1146.

Yan, W., Cao, Q.J., Arenas, R.B., Bentley, B., and Shao, R. (2010). GATA3 inhibits breast cancer metastasis through the reversal of epithelial-mesenchymal transition. J. Biol. Chem. *285*, 14042–14051.

Yao, Y.L., and Yang, W.M. (2003). The metastasis-associated proteins 1 and 2 form distinct protein complexes with histone deacetylase activity. J. Biol. Chem. *278*, 42560–42568.

Yoon, N.K., Maresh, E.L., Shen, D., Elshimali, Y., Apple, S., Horvath, S., Mah, V., Bose, S., Chia, D., Chang, H.R., and Goodglick, L. (2010). Higher levels of GATA3 predict better survival in women with breast cancer. Hum. Pathol. *41*, 1794–1801.

Zhang, Y., LeRoy, G., Seelig, H.P., Lane, W.S., and Reinberg, D. (1998). The dermatomyositis-specific autoantigen Mi2 is a component of a complex containing histone deacetylase and nucleosome remodeling activities. Cell *95*, 279–289.

Zhang, H., Stephens, L.C., and Kumar, R. (2006). Metastasis tumor antigen family proteins during breast cancer progression and metastasis in a reliable mouse model for human breast cancer. Clin. Cancer Res. *12*, 1479–1486.